communications biology

A Nature Portfolio journal

Article

https://doi.org/10.1038/s42003-025-08055-2

The role of *ladderlectin* in spermatogenesis and ovarian sperm storage in the black rockfish (*Sebastes schlegelii*)

Ruiyan Yang, Na Wang, Weihao Song ✉, Fengyan Zhang, Xiangyu Gao, Hao Sun, Tianci Nie, Gongchen Liu, Mengda Du, Fuxiang Liu, Hang Zhang, Jie Qi & Yan He ✉

Ladderlectin, a teleost-specific C-type lectin, has been primarily associated with innate immune defense. However, this study unveils an important role of *ladderlectin* in the reproductive processes of *Sebastes schlegelii*. Seven *ladderlectin* genes (*SscLL*s) are identified, with *SscLL3604* and *SscLL3605* exhibiting high testis-specificity expression. Both genes contain a C-type lectin domain (CTLD) and two carbohydrate-binding motifs (QPD and WSD), with *SscLL3605* also containing a signal peptide. Notably, SscLL3604 is predominantly cytoplasmic, while SscLL3605 is found both in the cytoplasm and cell membrane. Additionally, *SscLL*s are primarily localized in Sertoli cells at the mRNA level but also exist in spermatids and spermatozoa at the protein level. Further analysis reveals that SscLLs are present in sperm heads and can bind to ovarian cells, hinting at a pivotal role in long-term sperm storage in ovaries. Knockdown of *SscLL*s in vitro demonstrates their critical role in maintaining Sertoli cells and Leydig cells within the testis. Finally, inhibition of glycosylation or treatment with antibody of SscLLs leads to an increased incidence of embryonic malformation in *S. schlegelii*. These findings suggest that *ladderlectin* may also play an important role in the regulation of reproductive processes, thereby providing an additional adaptive mechanism for the reproduction of viviparous fish.

C-type lectins (CTLs), functioning as indispensable calcium-dependent carbohydrate-binding proteins, play pivotal roles in a wide range of biological processes, including innate immunity, cell-cell interactions, and developmental processes, in both animals and plants[1]. In teleost fish, C-type lectins are essential components of the innate immune system, functioning as pattern recognition receptors (PRRs) that detect and bind pathogen-associated molecular patterns (PAMPs) to initiate immune responses[2]. Their diverse nature and widespread distribution make them important players in the defense against pathogens and contribute to the overall health and survival of these aquatic organisms[3]. In addition to their well-established roles in immunity, emerging evidence suggests that C-type lectins may have multifunctional roles beyond pathogen recognition and clearance, such as spermatogenesis, ovarian sperm storage, and fertilization[4,5]. Although lectins like fucose-binding lectin bindin protein in *Crassostrea gigas* and Galectin-3 on sperm surfaces have been shown to facilitate fertilization[6–9], the exact function in teleost fish remains to be explored.

Ladderlectin, a distinct subgroup of CTLs, has a C-type lectin domain (CTLD) and exhibits carbohydrate-binding capacities, was initially purified from the serum and plasma of *Oncorhynchus mykiss* and named for its characteristic ladder-like appearance under unreduced SDS-PAGE conditions[10]. *Ladderlectin*s have garnered significant attention for their crucial roles in teleost fish immune systems[11–14]. Based on its physical and chemical properties as glycoprotein, ladderlectin protein exhibited calcium-dependent binding to Sepharose, lipopolysaccharide *of Aeromonas salmonicida*[15], various intact fish pathogens[11], and viral hemorrhagic septicemia virus (VHSV) IVb[16]. As a prototypical CTL, current understanding primarily focuses on its crucial involvement in recognizing and combating pathogens, yet the extent of its functional diversity remains unexplored. Investigating whether *ladderlectin* participates in additional physiological or

MOE Key Laboratory of Marine Genetics and Breeding, College of Marine Life Sciences/Sanya Oceanographic Institution, Ocean University of China, Qingdao/Sanya, China. ✉e-mail: songweihao8@163.com; yanhe@ouc.edu.cn

developmental processes could yield further insights into the complex regulatory networks governing fish health and well-being.

The black rockfish (*Sebastes schlegelii*), a viviparous marine teleost, exhibits complex reproductive strategies including internal fertilization, prolonged sperm storage, and intraovarian embryonic development[17–19]. Despite the ecological and economic importance of this species, the molecular mechanisms underlying these unique reproductive adaptations remain largely unexplored. In recent years, there has been growing interest in the potential role of proteins traditionally associated with immune functions in reproductive processes[20]. It is plausible that *ladderlectin*s, traditionally associated with immune functions, may also play a role in these reproductive mechanisms. Investigating whether *ladderlectin*s participate in the reproductive biology of *S. schlegelii* could provide valuable insights into the molecular mechanisms underlying its unique reproductive strategies and reveal additional aspects of functional diversification in teleost fish.

In this study, we investigated the functions of two testis-restricted expressed *ladderlectin* genes *SscLL3604* and *SscLL3605*, in *S. schlegelii*. We found they support Sertoli and Leydig cells in the testis and bind to ovarian cells of *S. schlegelii*. Blocking SscLLs on the sperm surface for artificial insemination, negligible effects were found on fertilization rates, yet resulted in an increased ratio of embryonic malformation. Our study provides valuable insights into the function of *ladderlectin* and a meaningful adaptive mechanism for the reproduction of viviparous fish.

Results

Bioinformatic analysis of *SscLL* genes

Based on genomic and transcriptomic data of *S. schlegelii*, seven *SscLL*s were identified through BLAST analysis using *ladderlectin* sequences from other species downloaded from NCBI (Supplementary Table S1). The coding sequences of the seven *SscLLs* varied significantly in length, with *SscLL3604* being the shortest at 369 bp, while *SscLL8355* being the longest at 624 bp. Sequence alignment revealed an identity of 75% among *SscLL0748, SscLL3603, SscLL3604*, and *SscLL3605*, with all containing the carbohydrate-binding motifs QPD and WSD (Fig. 1a). SMART analysis indicated a classic CLECT domain in all identified SscLLs. Notably, a signal peptide was also predicted at the N-terminal, suggesting that they are likely to be secretory proteins with the exception of SscLL3604 (Fig. 1c, d). Additionally, structural predictions conducted using AlphaFold3 revealed significant 3D structural variations among the SscLLs. Specifically, SscLL0748, SscLL3603, SscLL3604, and SscLL3605 each consisted of two α-helices, five β-sheets, and several random coils. In contrast, SscLL8354 and SscLL8356 each featured two α-helices and two β-sheets, while SscLL8355 comprised two α-helices and eight β-sheets. These structural differences suggest divergence in functional roles among the seven SscLLs (Fig. 1e). Phylogenetic analysis of *ladderlectin*s from various teleost fish based on amino acid sequences demonstrated that *ladderlectin*s from the same species clustered together, independent of their expression patterns (Fig. 1b and Supplementary Fig. S1). Notably, *ladderlectin*s from viviparous species, including *S. schlegelii*, *S. umbrosus*, *Poecilia reticulata*, and *Xiphophorus maculatus*, were found to form at least two distant branches, whereas *ladderlectin*s from oviparous species (*Danio rerio*, *O. mykiss*, *Gasterosteus aculeatus*, and *Oryzias latipes*) clustered into a single group. Additionally, synteny analysis of all identified *ladderlectin* genes revealed that only *ladderlectin* genes within the same clade were conserved, and the upstream regulatory region of these genes also displayed conserved sequences (Supplementary Fig. S2). We propose that the presence of two distinct clusters of *ladderlectin* genes in viviparous fish, as opposed to a single cluster in oviparous species, may be linked to the evolutionary adaptations associated with viviparity. Specifically, we hypothesize that *ladderlectin* genes in viviparous fish have evolved additional functions, such as mediating ovarian sperm storage, beyond their traditional roles in the immune system to support viviparous reproduction.

Expression analysis of *SscLL*s

We then investigated the expression patterns of the seven *SscLL*s using published transcriptome data[17]. Intriguingly, *SscLL0748* and *SscLL3603* exhibited high expression levels in the gill, *SscLL8354*, *SscLL8355*, and *SscLL8356* were predominantly expressed in the intestine, while *SscLL3604* and *SscLL3605* showed remarkable expression in the testis (Fig. 2a). As ladderlectins are known immune-related proteins[21], their elevated expressions in immune organs like gill and intestine are expected. However, the significant expression of *ladderlectin*s in the testis warrants further investigation. Therefore, our subsequent experiments focused on the functional roles of *SscLL3604* and *SscLL3605* in the testis of *S. schlegelii*. The tissue distribution of *SscLL3604* and *SscLL3605* at the transcriptional level was examined by PCR. Results showed that *SscLL3604* and *SscLL3605* transcripts were detected only in testis (Fig. 2b), which was consistent with the result of transcriptome data. To further verify the subcellular localization of SscLL3604 and SscLL3605, we constructed two recombinant plasmids, pEGFP-N1-SscLL3604 and pDsRed2-N1-SscLL3605, which were co-transfected into HEK293T cells (Fig. 2c). Fluorescence microscopy revealed that SscLL3604 predominantly localized to both the nucleus and cytoplasm, whereas SscLL3605 exhibited a primary localization in the cytoplasm and cell membrane. This differential localization may be attributed to the presence of a signal peptide in SscLL3605, which SscLL3604 lacks.

The spatial expression of *SscLL*s genes mRNA and protein in the testis of *S. schlegelii*

To elucidate the spatial expression patterns of *SscLL3604* and *SscLL3605* at the mRNA level, we performed in situ hybridization (ISH) analysis on the testis of *S. schlegelii* at different developmental stages (Fig. 3a–p). The testes were sampled during three distinct periods: the regressed stage, the regenerating stage, and the spermatogenesis stage. The results indicated that *SscLL3604* and *SscLL3605* displayed the same location, continuously expressed in Sertoli cells across all stages. This finding aligns with the results obtained from the single-cell transcriptome analysis of *S. schlegelii* testis (Supplementary Fig. S3)[22]. To investigate the biological functions of SscLL3604 and SscLL3605, recombinant proteins with Maltose Binding Protein (MBP) tag were expressed and purified using a prokaryotic expression system. Western blot (WB) using an anti-MBP primary antibody revealed a specific band at 55 kDa, which corresponds to the expectation (Supplementary Fig. S4). Enzyme linked immunosorbent assay (ELISA) results further demonstrated that the expressed proteins exhibited the characteristic carbohydrate-binding capacity of lectins (Supplementary Fig. S5). Due to the high sequence identity between SscLL3604 and SscLL3605, the recombinant proteins were then used as mixed antigens for anti-rSscLL mouse polyclonal antibody preparation. To observe the expression localization of SscLLs at the protein level, anti-rSscLL mouse polyclonal antibody was employed for immunohistochemistry (IHC) on the testis of *S. schlegelii*. We assessed SscLLs localization across three developmental stages of the testis, revealing specific expression in Sertoli cells at all stages except the spermatogenesis stage (Fig. 3q, r), which was consistent with the results of ISH (Fig. 3a–p). Notably, at the spermatogenesis stage, distinct yellow-brown signals were also observed in certain spermatids and spermatozoa (Fig. 3s, t), indicating a potential role for SscLLs in sperm function.

Effect of *SscLL*s genes knockdown on testis tissue blocks

To further investigate the function of *SscLL3604* and *SscLL3605* in testis development, we performed in vitro culture of testis tissue blocks from *S. schlegelii*. Subsequently, we conducted in vitro knockdown experiments, precisely targeting these genes to unravel their specific contributions to the developmental process. qRT-PCR results indicated that after siRNA treatment, expression levels of *SscLL3604* and *SscLL3605* in the testis tissue blocks decreased by approximately 75% and 67%, respectively (Fig. 4a, b). Then, Hematoxylin and Eosin (H&E) staining was performed to investigate the effect of *SscLL3604* and *SscLL3605* knockdown on testis morphology. The results showed that after *SscLL3604* and *SscLL3605* knockdown, there was a significant reduction in the number of

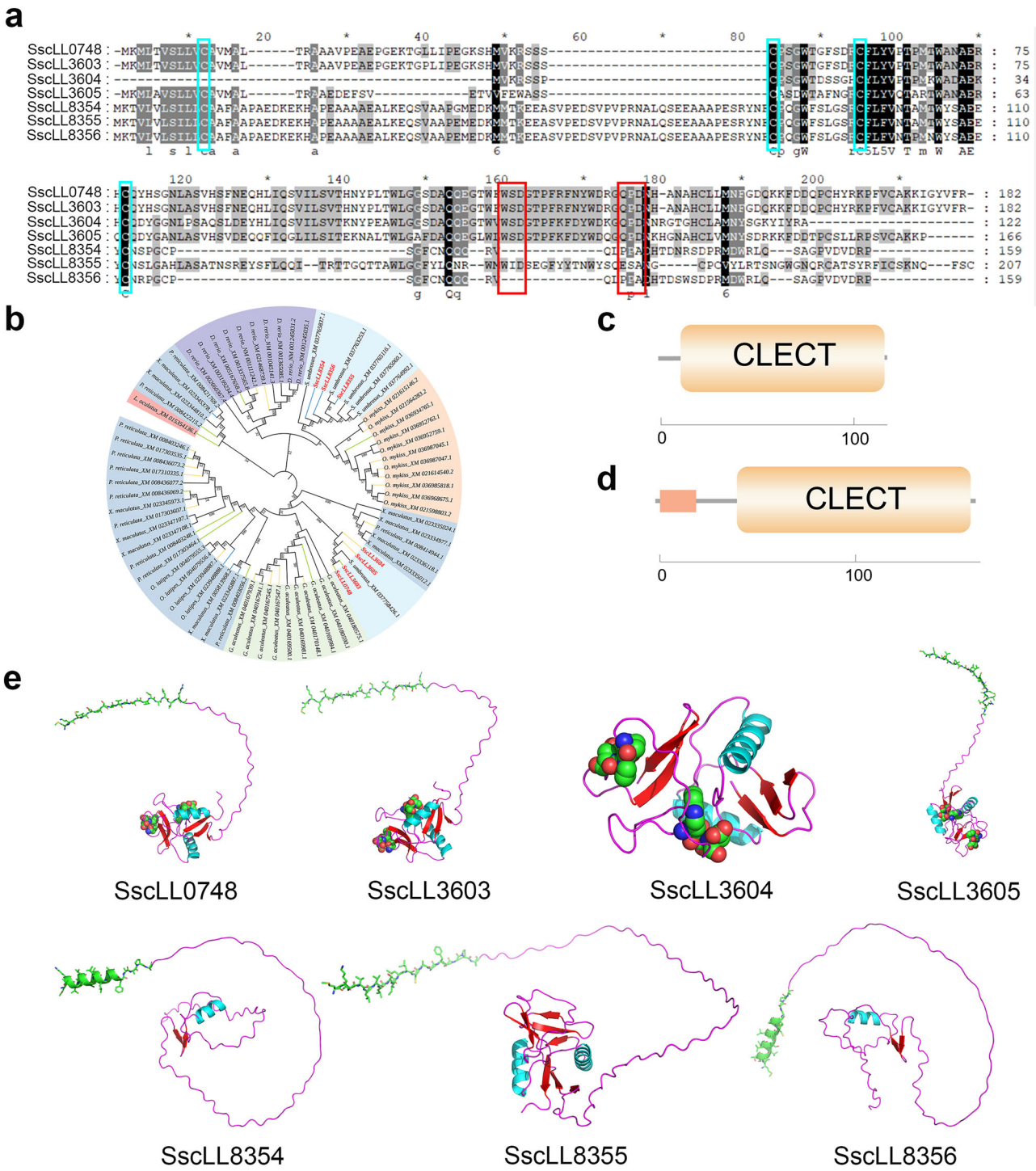

Fig. 1 | Bioinformatic analysis of *SscLLs*. a Amino acid sequences alignment of seven SscLLs. Black shadows represent the same residues, and gray shadows represent similar residues. The carbohydrate-binding motifs QPD and WSD are marked with red boxes, and the conserved cysteine residues that formed two pairs of disulfide bonds are shown in blue boxes. **b** Phylogenetic analysis of *ladderlectins* from various teleost fish. *SscLLs* were marked by red shadows, the accession numbers of *ladderlectins* from other species were shown in the pictures, and the numbers next to the internal branches indicate the bootstrap values based on 1000 replications. The color of branches represents the tissue expression specificity of *ladderlectins*, orange—testis, green—gill, blue—intestine, and black—other tissues. **c** Schematic of protein motifs of SscLL3604, which is the only one that does not contain a signal peptide. **d** Schematic of protein motifs of other SscLLs, with the signal peptide represented by an orange rectangle, and the lectin domain indicated with a rounded rectangle. **e** Tertiary structure of SscLLs. The signal peptides are shown with the stick model, the carbohydrate-binding motifs are shown with the spheres model, and the rest are shown with the cartoon model. Blue indicates α-helix, red indicates β-sheet, and random coil is marked with purple.

Sertoli cells and Leydig cells surrounding the seminal vesicles compared to the NC group. This decrease compromised the structural integrity and resulted in loosened connections between the seminal vesicles (Fig. 4f). We performed quantitative detection of marker genes for Sertoli cells and Leydig cells. The qRT-PCR results showed that the expression levels of the Sertoli cell marker genes *comt* and *cystatin*, as well as the Leydig cell marker gene *insl3*, were significantly downregulated following the knockdown of the expression of *SscLL3604* and *SscLL3605* genes

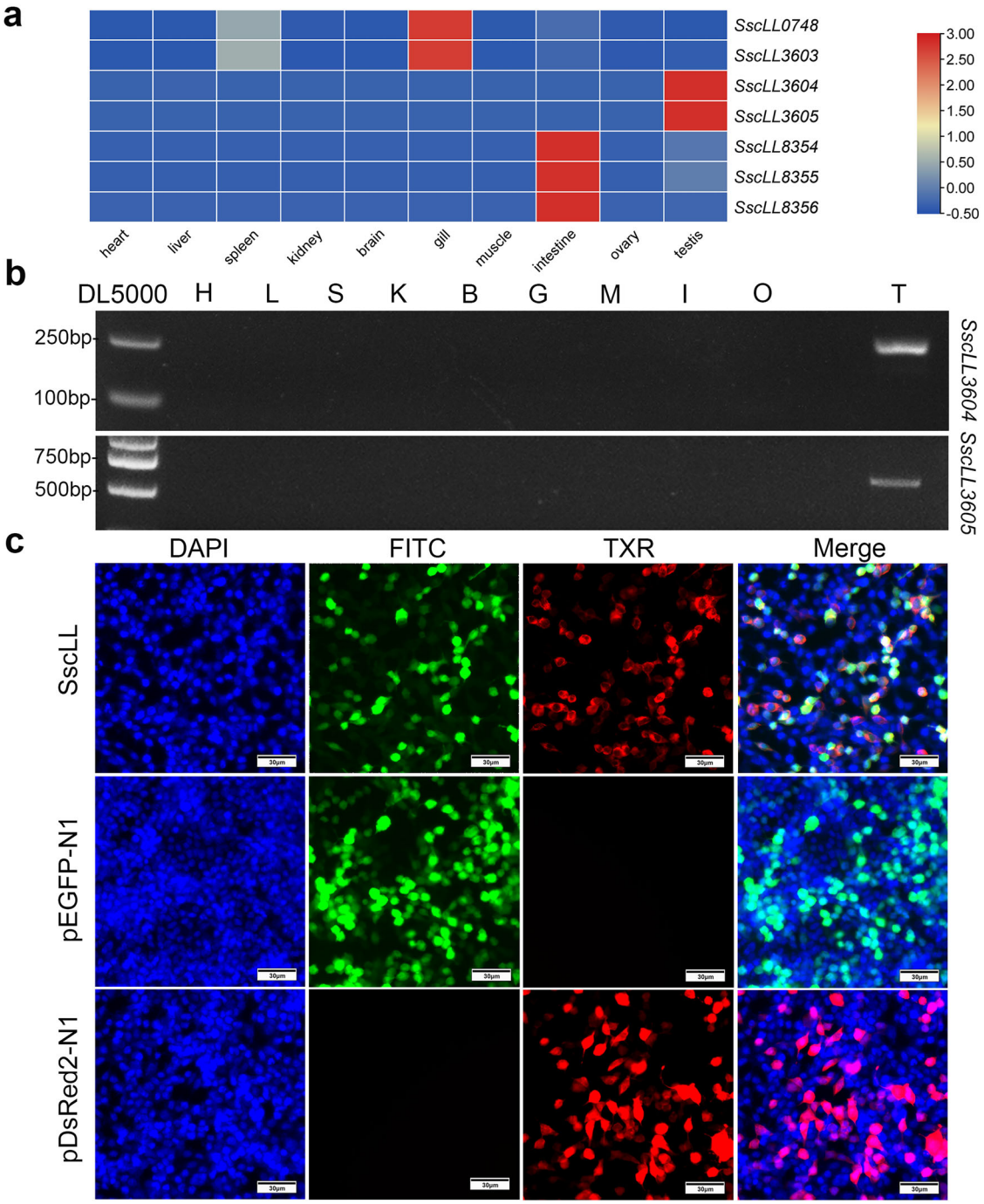

Fig. 2 | SscLLs expression in different tissues of *S. schlegelii* and subcellular localization in HEK293T cells. a Heatmap of the expression of *SscLL*s. The horizontal axis represents each tissue of *S. schlegelii*, the vertical axis represents the gene IDs, and the scale bar indicates the normalized TPM value. **b** PCR products of *SscLL3604* and *SscLL3605* gene fragments in different tissues of *S. schlegelii*. H heart, L liver, S spleen, K kidney, B brain, G gill, M muscle, I intestine, O ovary, T testis. **c** Subcellular localization of pEGFP-N1-SscLL3604 and pDsRed2-N1-SscLL3605. The nucleus of HEK293T cells were stained with DAPI, the green fluorescence represented pEGFP-N1-SscLL3604 or pEGFP-N1, and the red fluorescence represented pDsRed2-N1-SscLL3605 or pDsRed2-N1. Scale bars, 30 μm.

(Fig. 4c–e). Considering the specific expression of *SscLL*s in Sertoli cells, we inferred that their expression is closely related to the maintenance of Sertoli cells in the testis, and further affects the maintenance of Leydig cells.

Existence of SscLLs in spermatozoa of *S. schlegelii* and their binding to ovarian cells

Based on the results of IHC in the spermatogenesis stage, we further confirmed the existence of SscLLs in spermatozoa by WB and immunofluorescence (IF) analyses using the anti-rSscLL mouse polyclonal antibody referred to above (Fig. 5b–e). The WB results displayed a single band at 15 kDa, which indicated the existence of SscLLs in sperm (Fig. 5e). Additionally, the IF analysis revealed the location of SscLLs on sperm heads (Fig. 5b, c), which potentially indicated the crucial role of SscLLs in zona pellucida binding[23]. To further confirm the importance of SscLLs in sperm storage or sperm-oocyte recognition, the rSscLLs protein was incubated with ovarian cells in vitro to detect their binding capacity. WB results indicated their detectable binding capacity with

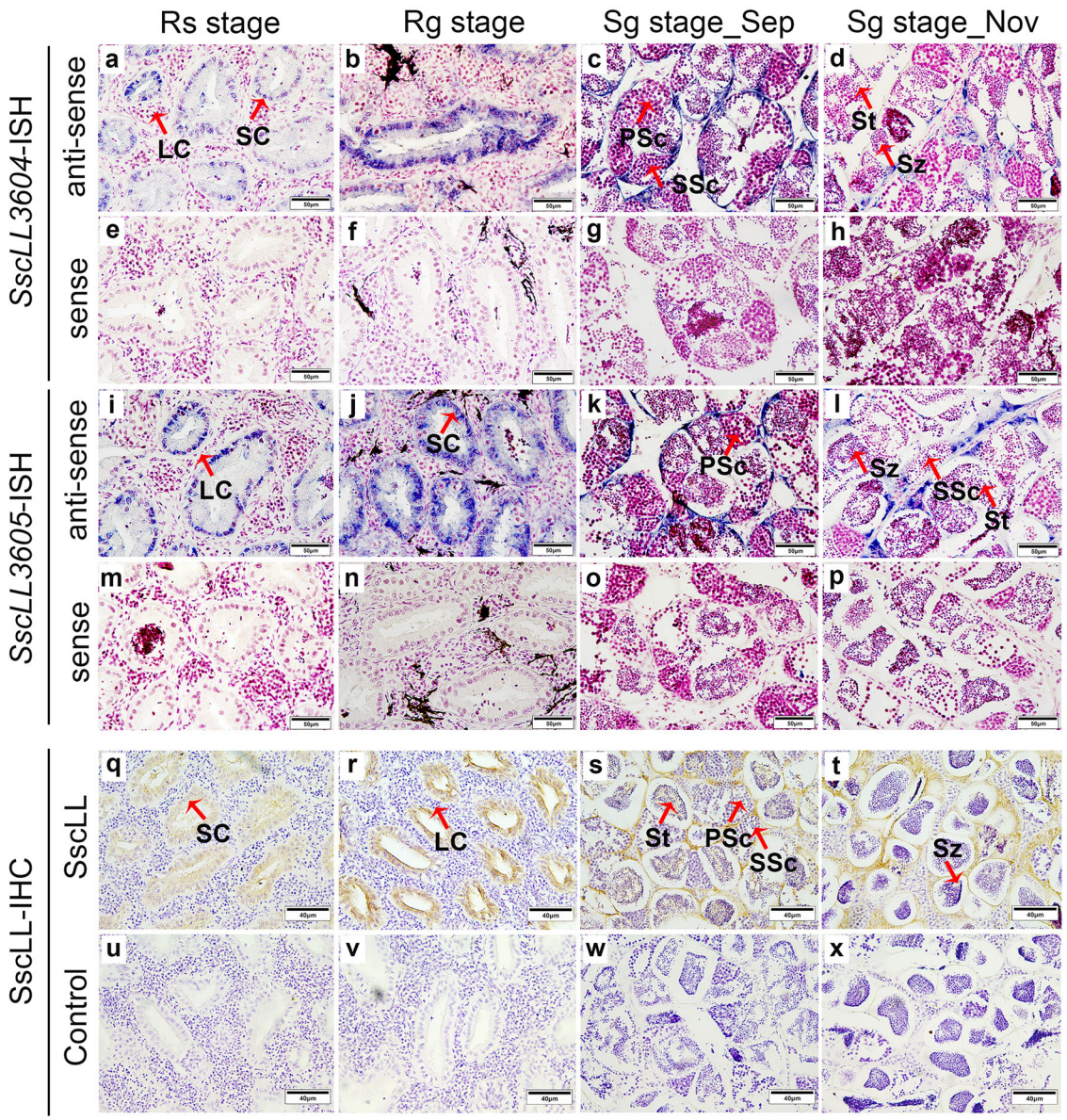

Fig. 3 | The spatial expression of *SscLLs* genes mRNA and protein in *S. schlegelii* testis at different developmental stages during the annual reproductive cycle. a–p Localization of *SscLL3604* and *SscLL3605* gene mRNA by ISH. Positive signals from hybridization with antisense probes are shown in blue, and negative signals from hybridization with sense probes are uncolored. **q–x** The spatial expression of SscLLs protein using IHC. The positive signal of IHC was shown to be yellow-brown, and the negative control tissues were stained blue with hematoxylin. Rs stage Regressed Stage, Rg stage Regenerating Stage, Sg stage_Sep Spermatogenesis Stage in September, Sg stage_Nov Spermatogenesis Stage in November, PSc Primary spermatocytes, SSc Secondary spermatocytes, St Spermatid, Sz Spermatozoa, LC Leydig cell, SC Sertoli cell. Scale bars, 50 μm, 40 μm.

ovarian cells in a concentration-dependent manner (Fig. 5f). However, dual-color immunofluorescent analysis revealed that rSscLLs protein predominantly binds ovarian somatic cells (Fig. 5a). Besides, the results of in vitro incubation showed that sperm treated with anti-rSscLL mouse polyclonal antibody failed to bind to ovarian cells, whereas sperm treated with D-fructose, D-galactose, and D-mannose exhibited varying degrees of binding (Supplementary Fig. S6). These findings confirm that sperm bind to ovarian cells via the SscLLs protein, highlighting its crucial role in long-term storage within the ovary.

SscLLs are involved in the long-term ovarian sperm storage and embryonic development process of *S. schlegelii*

After copulation, the sperm are stored in the ovaries for about 5 months in *S. schlegelii*. During this period, the spermatozoa are not in a resting state. Previous studies indicate that in January, sperm are predominantly located in the crypt surrounded by germinal epithelium and follicular layer. By February, sperm gradually migrate towards the outer granulosa cells[18]. To further investigate the impact of SscLLs on sperm storage, we blocked the SscLLs protein on sperm with anti-rSscLL mouse polyclonal antibody or glycosylation inhibitors such as tunicamycin and Benzyl-α-GalNAc, which can inhibit the glycosylation process of SscLLs (Fig. 6).

In January, five individuals from each group were sampled for sperm detection. In the control group, spermatozoa were detected in 4/5 individuals and were freely situated in the crypt, which was the same as the previously reported case. In the other three groups, the observed spermatozoa displayed the same status as the control group. While the number of sperm-detectable individuals seems different as 2/5 in the tunicamycin treatment group, 4/5 in the Benzyl-α-GalNAc treatment group, and 3/5 in the antibody treatment group. By February, the spermatozoa were detectable in 3/5 individuals in the control group, 3/5 in the tunicamycin

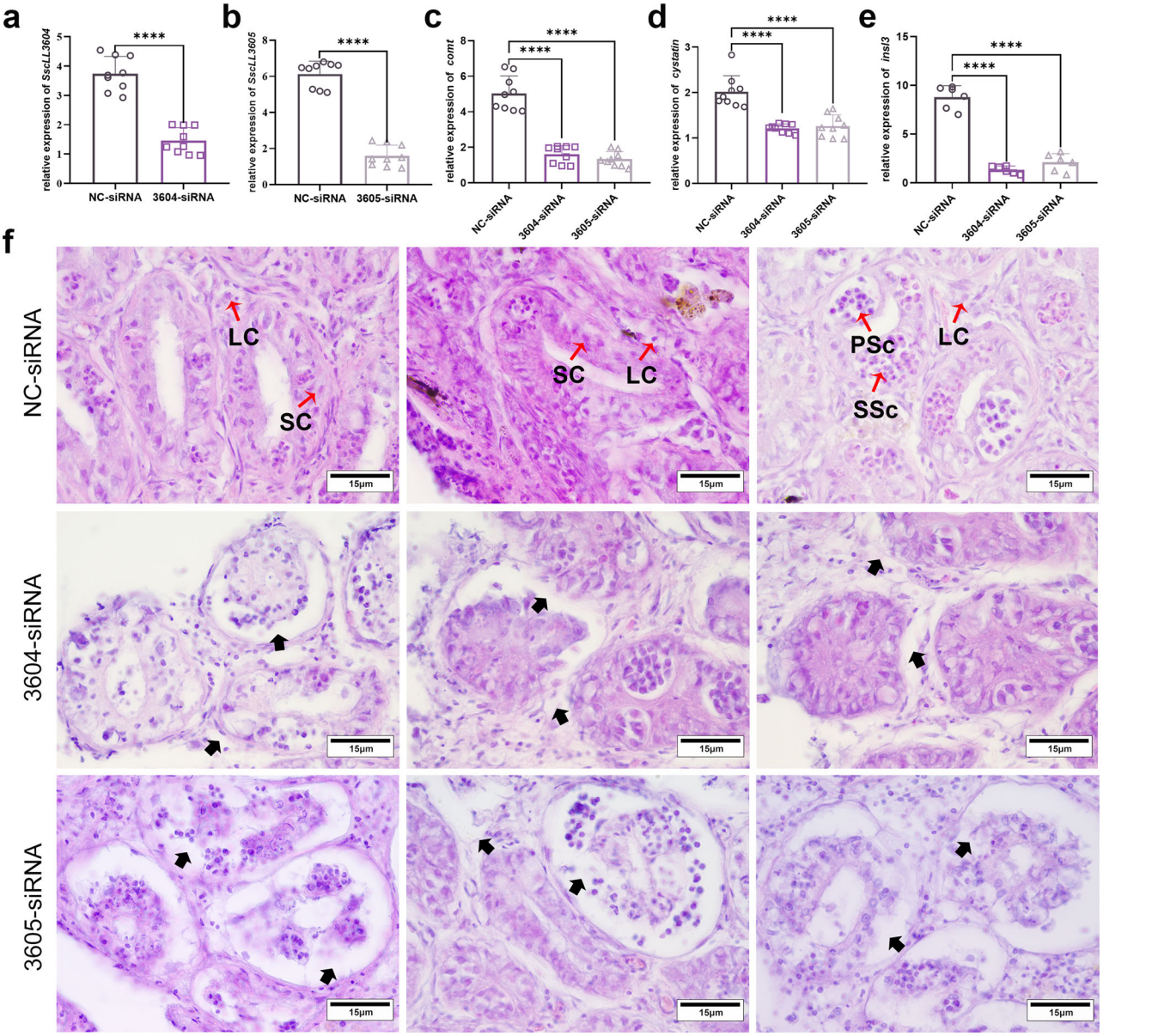

Fig. 4 | The effect of *SscLL3604* and *SscLL3605* knockdown on testis tissue blocks. **a**, **b** Temporal mRNA expression levels of *SscLL3604* and *SscLL3605* were detected by qRT-PCR in testis tissue blocks treated by 3604-siRNA and 3605-siRNA ($n = 9$). *Rpl17* was used as the internal control. **c**, **d** The expression level of Sertoli cell marker genes in *SscLL3604* and *SscLL3605* gene knockdown testis tissue blocks ($n = 9$). **e** The expression level of the Leydig cell marker gene in *SscLL3604* and *SscLL3605* gene knockdown testis tissue blocks ($n = 6$). $^{****}P < 0.0001$ as assessed using two-tailed Welch's *t* test analysis. Data in (**a**–**e**) are presented as mean ± standard deviation (SD). *n*, the number of parallel samples. **f** Histological observation of *SscLL3604* and *SscLL3605* gene knockdown testis tissue blocks, each group selected 3 representative images, black arrows indicate the representative phenotypes after siRNA treatment. PSc Primary spermatocytes, SSc Secondary spermatocytes, LC Leydig cell, SC Sertoli cell. Scale bars, 15 μm.

treatment group, 5/5 in the Benzyl-α-GalNAc treatment group, and 1/5 in the antibody treatment group. Remarkably, spermatozoa in the control group had dispersed to varying extents within the granular cell layer, agreeing with previous studies. However, in the other groups, some sperm were still stored in the crypt, indicating a delayed migration compared to the control group (Fig. 6a). This suggests that SscLLs have an impact on sperm storage within the ovary, particularly on sperm localization.

Before parturition in April, another five individuals from each group were sacrificed to further investigate the potential effect of SscLLs blocking on fertilization or embryonic development (Fig. 6b–h and Supplementary Table S5, 6, and the biological indicators of *S. schlegelii* are listed in Supplementary Table S7). Firstly, we statistically analyzed the fertilization rates among four groups. The results indicated that a significant reduction in fertilization rates was observed exclusively in the Benzyl-α-GalNAc treatment group. In contrast, no significant differences were found in the tunicamycin or antibody treatment groups compared to the control group (Fig. 6e). These findings suggested that while all three treatment groups alter the position of sperm storage within the ovary, only the inhibition of O-glycosylation (as affected by Benzyl-α-GalNAc) impacts fertilization rates. The tunicamycin and antibody treatments, although modify sperm storage location, do not affect the fertilization process. Furthermore, we compared the embryonic development among the groups. Significantly, the control group exhibited a high normal embryo development rate of 95%, which was significantly higher than the other three groups with 50% in the tunicamycin or Benzyl-α-GalNAc treatment groups, and 75% in the antibody treatment group (Fig. 6f). Moreover, both the incidence of defective (Fig. 6g) and undeveloped embryos (Fig. 6h) were significantly higher in the treatment groups compared to the control group. These results suggested

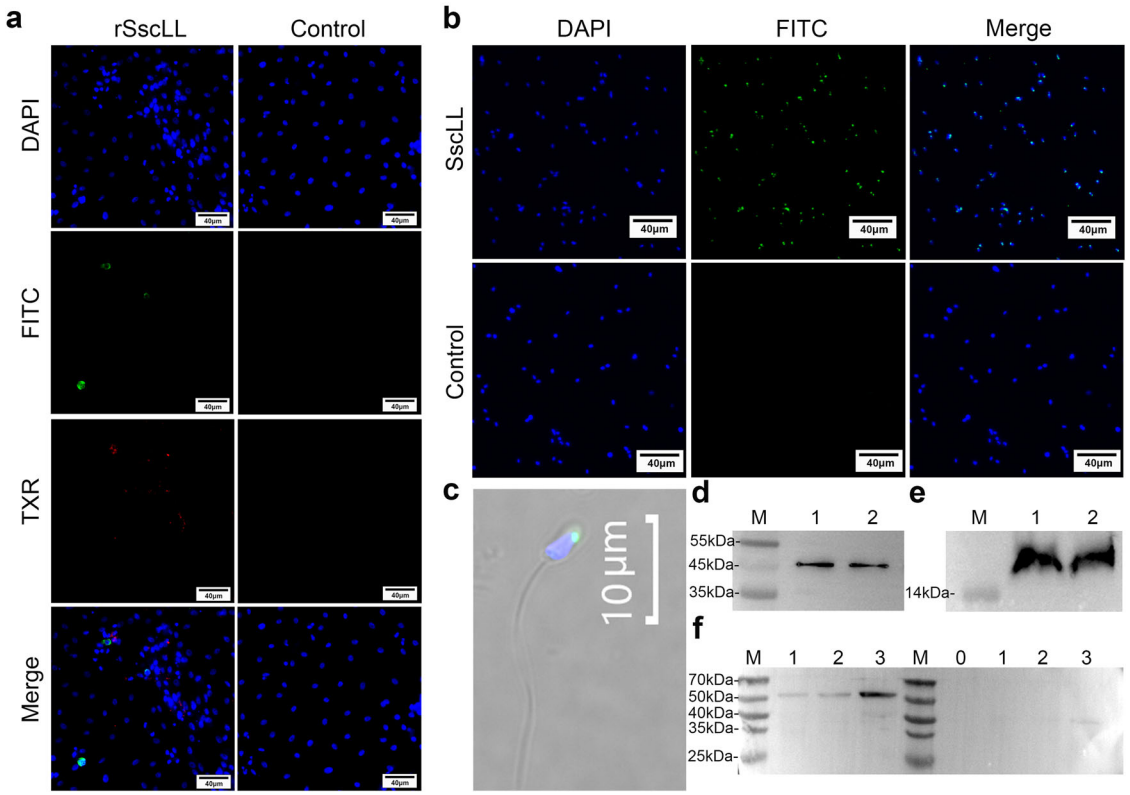

Fig. 5 | Detection of SscLLs on sperm of *S. schlegelii* and their binding to ovarian cells. a The ovarian nucleus is stained blue with DAPI. The germ cells showed green fluorescence with the polyclonal antibody against fish Vasa and YF® 488 Goat Anti-Rabbit IgG. The rSscLLs protein binding to ovarian cells presented red fluorescence by using the anti-rSscLL mouse polyclonal antibody and the YF® 594 Goat Anti-Mouse IgG. Scale bars, 40 μm. **b**, **c** Sperm nucleus was stained in blue with DAPI, and the SscLLs were stained in green with FITC. We made higher-resolution images under oil immersion microscopy. Scale bars, 40 μm, 10 μm. **d**, **e** Detection of SscLLs on sperm of *S. schlegelii* by WB using anti-β-actin antibody and anti-rSscLL mouse polyclonal antibody, two lanes represent two parallel individuals. β-actin was used as a positive control for protein presence. **f** Detection of the binding of rSscLLs with ovarian cells of *S. schlegelii* by WB using the anti-MBP primary antibody. M: protein marker; Lane 0: Ovarian cells only, not incubated with protein; Lane 1–3: The ovarian cells were incubated with 10 μg/mL (lane 1), 20 μg/mL (lane 2), and 40 μg/mL (lane 3) protein at 24 °C for 13 h.

that SscLLs blocking can hamper the normal sperm storage process and sperm localization, and the improper sperm storage within the ovary may have downstream effects on embryo development, even if fertilization rates remain largely unaffected.

Discussion

In this study, we identified seven *ladderlectin* genes in *S. schlegelii*, among which *SscLL3604* and *SscLL3605* exhibited high testis-specific expression. We demonstrated that these two *ladderlectin* genes are involved in the reproductive processes of *S. schlegelii*. While C-type lectins have been extensively studied for their roles in innate immunity as PRRs[11–14], our findings revealed an additional function for *ladderlectin*s in reproduction, particularly in spermatogenesis, ovarian sperm storage, and embryonic development.

Although *ladderlectin* was first purified in the serum and plasma of *O. mykiss*[10], followed by hybrid crucian carp[13], *Plecoglossus altivelis*[12], and *Larimichthys crocea*[14], there seems no systematic evolutionary analysis reported yet. Herein, we conducted a comprehensive evaluation of *ladderlectin* genes across various teleost fish, aiming to address this gap. Phylogenetic tree analysis indicated the exclusive presence of the *ladderlectin* genes within teleost fish, revealing their unique evolutionary status and suggesting a potential correlation to species-specific physiological adaptations, which corresponds to the conclusions of Tang[14]. Obviously, all the surveyed teleost fish possess multiple *ladderlectin* genes except *Lepisosteus oculatus*, an outgroup for the teleost genome duplication[24]. This finding, coupled with the variable gene numbers and intricate synteny patterns, hints at a rapid evolutionary trajectory following the third whole-genome duplication, possibly indicating functional diversification among *ladderlectin* genes. Furthermore, the clustering of *ladderlectin* genes according to species/lineages reveals distinct and independent evolutionary trajectories, emphasizing their uniqueness across teleost fish. Adapted to their function, *ladderlectin* genes were predominantly expressed in immune organs such as branchial epithelium, hepatic sinusoids, and intestinal submucosal granular layer[14]. In *S. schlegelii*, most *SscLL*s were predominantly expressed in immune-related tissues as expected, such as the gill and intestine, which was consistent with previous studies[12–14,25]. Intriguingly, two *SscLL*s, *SscLL3604* and *SscLL3605*, exhibit significantly higher expression in the testis, challenging conventional notions regarding *ladderlectin* gene expression patterns and suggesting an additional role in the reproductive system. Thus, the specific role of *SscLL3604* and *SscLL3605* was explored here. Structural analysis showed that both genes contain typical C-type lectin-like domains (CTLDs) and conserved carbohydrate-binding motifs (QPD and WSD), implicating them in carbohydrate-mediated interactions[26,27], and inspiring us that the function of *ladderlectin* may be demolished by interfering with their glycosylation process[28]. Notably, *SscLL3605* also possesses a signal peptide, suggesting its involvement in secretory pathways[29]. Subcellular localization studies demonstrated that SscLL3604 is predominantly cytoplasmic, while SscLL3605 localizes to both the cytoplasm and cell membrane. This differential localization hints at distinct but potentially complementary roles in testicular function and sperm maturation. In addition, our study demonstrated that there were also *ladderlectin*s displaying testis-specific expression in *G. aculeatus*, *O. latipes*, *P. reticulata*, and *O. mykiss*, besides *S. schlegelii*, which can serve as a new example of convergent evolution. Besides, the regulatory mechanism behind their testis-

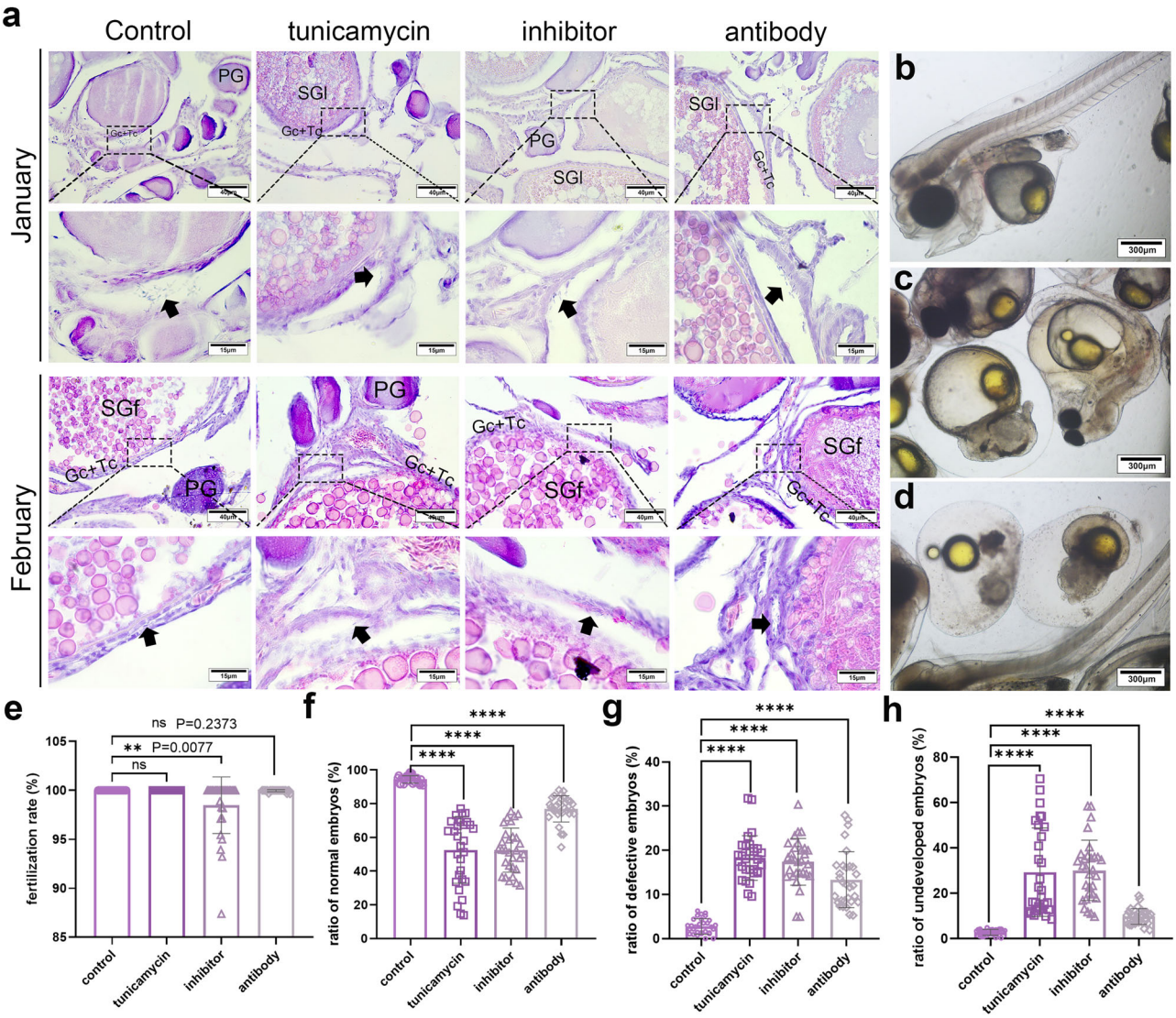

Fig. 6 | The effects of SscLLs in the long-term ovarian sperm storage and embryonic development process of *S. schlegelii*. **a** Movement trajectories of sperm within the ovaries of *S. schlegelii* in control and experimental groups at different time points. Black arrows indicate spermatozoa. PG Oocyte at the 2 phase (primary growth), SGl Oocyte at the 4 phase (late secondary growth), SGf Oocyte at the 5 phase (full secondary growth), Gc granulosa cell, Tc theca cell. Scale bars, 40 μm, 15 μm. **b–d** Representative embryos photographed under the microscope. Scale bars, 300 μm. **e** Comparison of fertilization rates between the control group and the experimental group ($n_{control}$ = 7208; $n_{tunicamycin}$ = 6093; $n_{inhibitor}$ = 5286; $n_{antibody}$ = 7320, and the detailed data are listed in Supplementary Table S5. *n*, the total number of fertilized and unfertilized eggs counted). The ratio of normal embryos (**f**), defective embryos (**g**), and undeveloped embryos (**h**). Vertical bars represent the mean ± SD ($n_{control}$ = 7208; $n_{tunicamycin}$ = 6093; $n_{inhibitor}$ = 5231; $n_{antibody}$ = 7317, and the detailed data are listed in Supplementary Table S6. *n*, the total number of embryos counted), and the horizontal axis represents different groups. ****$P < 0.0001$ as assessed using two-tailed Welch's *t* test.

specific expression pattern and the convergence of *ladderlectin* function in testis among various species remains to be further explored.

The in situ hybridization and immunohistochemistry analyses revealed that *SscLLs* are primarily expressed in Sertoli cells at the mRNA level and in spermatids and spermatozoa at the protein level. Sertoli cells are essential for supporting and nurturing developing germ cells during spermatogenesis[30]. The presence of *SscLLs* in these cells suggests that *ladderlectins* may participate in the regulation of the germ cell microenvironment[31]. The detection of SscLLs in spermatids and spermatozoa indicates a potential role in sperm maturation and function[32]. During mammalian fertilization, the sperm head initiates recognition by binding Galectin-3 to the zona pellucida[8]. The acrosomal reaction remodels the sperm head, enabling fusion proteins (IZUMO1[33], SPACA6[34], TMEM95[35], and FIMP[36]) to migrate to the equatorial region, facilitating membrane fusion and genetic material exchange. Interestingly, we found that SscLLs proteins are present on the heads of spermatozoa and are capable of binding to ovarian cells. This observation implies that ladderlectins may facilitate the long-term storage of sperm within the ovary, as well as subsequent sperm-egg recognition and binding, which are processes critical for successful fertilization in viviparous fish. And similar mechanisms may exist in *S. schlegelii*, with ladderlectins contributing to the specificity and efficiency of fertilization. Viviparous teleosts like *S. schlegelii* are known to store sperm for extended periods before fertilization occurs[17]. The binding of ladderlectins to ovarian cells could help maintain sperm viability and readiness for fertilization when oocyte maturation is complete. This function would represent a crucial adaptation facilitating internal fertilization and successful reproduction in this species. The in vitro knockdown of *SscLLs* resulted in the compromised maintenance of Sertoli and Leydig cells in the testis. Leydig cells produce testosterone, which is essential for spermatogenesis and secondary sexual characteristics[37,38]. The disruption of these cell types upon *SscLLs* knockdown underscores the importance of *ladderlectins* in testicular function and hormonal balance. It suggests that *ladderlectins* may influence

the endocrine environment necessary for normal spermatogenesis[39]. Our treatments with antibody and inhibitors were observed to alter the storage location of sperm within the ovaries. We hypothesized that misplacement of sperm would result in reduced fertilization rates. Consistent with this hypothesis, we observed a significant reduction in fertilization rates only in the Benzyl-α-GalNAc treatment group (98.49% versus 100% in control). Two key factors likely contribute to the statistical significance. First is the absolute consistency observed in the control group, as all 30 control replicates achieved 100% fertilization (zero variance), reflecting exceptional experimental stability. Second, the Benzyl-α-GalNAc treatment group exhibited a consistent downward trend. Although a slight variation was observed across replicates, fertilization rates in 10 out of 30 replicates were below 100%, giving rise to a 1.51% average reduction and highlighting a unidirectional influence of the inhibitor. However, no significant differences were detected in the antibody or tunicamycin treatment groups compared to the control group (Supplementary Table S5 and Fig. 6e). Importantly, we noted a significant increase in embryonic malformation rates across all treatment groups (Fig. 6). This finding suggests that improper sperm storage within the ovary may have downstream effects on embryo development, even though it appears to have only a minimal effect on fertilization rates. Embryo developmental status remains a vital indicator of sperm functionality, as mispositioned sperm may experience disruption in mRNA translation, chromatin remodeling, and epigenetic modifications. These alterations, in turn, can compromise proper embryogenesis and increase the likelihood of developmental abnormalities[40–44]. Moreover, the consistent increase in embryonic malformation rates across all treatment groups suggests that the observed effects are attributable to specific mechanisms related to sperm function rather than non-specific toxicity. Furthermore, SscLLs are specifically expressed in the testis, and the antibodies employed in our study lack binding targets in the ovary (Supplementary Fig. S3). This specificity indicates minimal, if any, direct impact of the antibodies on ovarian tissues or embryos. The precise mechanisms remain to be elucidated, but SscLLs likely participate in early cell signaling or provide structural support during embryogenesis. Further research is needed to clarify their exact functions and the underlying mechanisms.

Our study unveils the multifaceted roles of *ladderlectin*s in *S. schlegelii*, demonstrating their involvement in both immune defense and reproductive processes. This functional diversification underscores an adaptive mechanism tailored to the unique reproductive strategies of viviparous fish. Notably, the dual role of *ladderlectin*s aligns with the concept of gene pleiotropy, where a single gene can influence multiple phenotypic traits[45]. This pleiotropic nature of *ladderlectin*s could confer advantages to *S. schlegelii* in navigating diverse environmental challenges, fostering coordinated responses across immune and reproductive systems[46]. Evolutionarily, the integration of immune-related proteins in reproductive processes is not novel, highlighting the intricate interplay between these biological systems. The close interconnection between immune and reproductive systems is increasingly recognized, with immune molecules implicated in diverse processes including ovulation[47], implantation[48], and placental development[49] in mammals. Our findings extend this understanding, revealing that ladderlectins, previously regarded primarily as immune proteins, also play pivotal roles in reproduction in non-mammalian vertebrates, specifically *S. schlegelii*. Furthermore, our study underscores the crucial role of post-translational modifications, particularly glycosylation, in ladderlectin function. Inhibition of glycosylation resulted in developmental abnormalities, emphasizing the necessity of proper glycosylation for ladderlectin functionality. This finding is consistent with the broader understanding that glycosylation is critical for the stability, localization, and activity of many proteins[50]. Despite advancing our comprehension of *ladderlectin* roles in reproduction, several questions persist. Future research is warranted to elucidate the precise molecular mechanisms underlying *SscLLs*' influence on Sertoli and Leydig cells function. Moreover, the signaling pathways implicated in *ladderlectin*-mediated embryonic development remain to be clarified. Future studies utilizing techniques such as gene editing (e.g., CRISPR/Cas9) could provide deeper insights into the gene functions and regulatory networks involved.

In conclusion, our study unravels the multifaceted roles of *ladderlectin*s in *S. schlegelii*, encompassing both immune defense and reproductive processes, suggesting an evolutionary adaptation to its viviparous reproduction. This underscores intricate links between immune and reproductive systems in teleosts, enriching our knowledge of reproductive biology. Our findings have implications for fish breeding, conservation, and population management, and may inspire further strategies to enhance fish health and reproduction, with broader impacts on aquatic ecosystem conservation and management.

Methods

Fish recruitment and sampling

We have complied with all relevant ethical regulations for animal use. This study was approved by the College of Marine Life Sciences, Ocean University of China Institutional Animal Care and Use Committee, and all research and feeding animals were performed according to the guidelines of China Government Principles for the Utilization and protection of vertebrates. Thirty-six *S. schlegelii* (thirty males and six females) (body length: 28.5 ± 2.4 cm, body weight: 619.5 ± 166.2 g) at different developmental stages, which were used for in situ hybridization, immunohistochemistry, sperm collection, ovarian cell isolation, and testis tissue block knockdown were bought from the Nanshan Market in Qingdao, China. The live fish were transported from the market to the laboratory in oxygenated packaging bags for sample collection. For artificial insemination, 120 female *S. schlegelii* (body length: 33.3 ± 2.6 cm, body weight: 676.5 ± 223.5 g) were obtained from offshore cages located in the Huangdao district of Qingdao, China, with permission from the relevant authorities. These cages are medium-sized cages with a length and width of 5 m, and the water depth is 7–10 m. Four groups were set up: the control group, the tunicamycin treatment group, the Benzyl-α-GalNAc treatment group, and the anti-rSscLL mouse polyclonal antibody treatment group. The control group was injected with urine-diluted sperm through the genital pore, following the established protocols[51]. The tunicamycin treatment group received sperm injections combined with tunicamycin (lectin inhibitor, also N-glycosylation inhibitor) (T818567, Macklin, Shanghai) with a concentration of 2 mg/kg ovarian weight. The Benzyl-α-GalNAc treatment group was injected with sperm and Benzyl-α-GalNAc (O-glycosylation inhibitor, HY-129389, MCE, USA) also with a concentration of 2 mg/kg ovarian weight. Lastly, the anti-rSscLL mouse polyclonal antibody was co-injected with sperm at a concentration of 1.6 mg/kg ovarian weight to the anti-rSscLL mouse polyclonal antibody treatment group. During in vivo experiments, each *S. schlegelii* was randomly selected from the offshore cages, and implanted in the muscle with a unique electronic tag (MAI Vision Technologies Co., Ltd., Shanghai) bearing an identification number (e.g., 00000395XXXX). This tagging system allowed us to distinguish among experimental treatments as well as to track individual fish throughout the study. For ease of reference, we used the final four digits of each identification number to refer to specific individuals. Subsequently, artificial insemination was performed based on predetermined group arrangements, and the fish were returned to different cages for further breeding. Considering the alterations in sperm storage locations within the ovaries and the developmental stage of the ovaries[18], 20 females were randomly selected on January 27th and February 27th respectively. During sampling, a certain number of fish were randomly selected from each group, transported back to the laboratory in oxygenated packaging bags, and then anesthetized with MS-222 for dissection to obtain ovary or embryo samples. The remaining parts were disposed of in accordance with the standard protocols for animal carcass management. The ovaries were preserved in two parts, one part was fixed with 4% Paraformaldehyde Fix Solution (PFA) and used for H&E staining, following the detailed protocol described previously[18], and the other part was cut into small pieces, frozen with liquid nitrogen and stored at −80 °C, and then used for RNA extraction. In April, five fish were randomly selected from the remaining females in each group for fertility and embryo

development assessment. Each ovary was divided into six equal parts, from which at least 100 embryos were randomly collected for statistical analysis. To minimize bias and ensure the objectivity of our results, a blinded approach was implemented throughout the study. Specifically, the investigators responsible for data collection and analysis were blinded to the group allocation.

Gene identification and bioinformatics analysis

A set of *ladderlectin* mRNA sequences from 15 species (accession numbers are listed in Supplementary Table S1) were used as query sequences to blast the genome of *Branchiostoma floridae*, *Petromyzon marinus*, *Chiloscyllium plagiosum*, *L. oculatus*, *D. rerio*, *O. latipes*, *P. reticulata*, *X. maculatus*, *G. aculeatus*, *S. umbrosus*, *O. mykiss*, *S. schlegelii*, *Xenopus laevis*, *Zootoca vivipara*, *Gallus gallus*, *Mus musculus*, and *Homo sapiens* individually with a standard as identity >25%, evalue < 2E−5, and only transcripts >300 bp and <700 bp were retained. Finally, a total of 73 *ladderlectin* genes were identified only in teleost fish, including seven in *S. schlegelii* (namely *SscLL0748, SscLL3603, SscLL3604, SscLL3605, SscLL8354, SscLL8355, SscLL8356*), one in *L. oculatus*, ten in *D. rerio*, four in *O. latipes*, thirteen in *P. reticulata*, eleven in *X. maculatus*, ten in *G. aculeatus*, six in *S. umbrosus*, and eleven in *O. mykiss* (accession numbers listed in Supplementary Table S2). All the identified *ladderlectin* mRNA sequences were aligned using MUSCLE implanted in MEGA 7.0 with default parameters. The phylogenetic tree was constructed using Phylosuite's Maximum Likelihood method with 1000 bootstrap replicates[52] and visualized using iTOL (https://itol.embl.de/)[53]. In addition, we also downloaded transcriptomes from different tissues of the above species (accession numbers are listed in Supplementary Table S3) and calculated transcripts per kilobase million (TPM) values by Salmon v0.7.2[54] to evaluate the expression level of *ladderlectin* genes.

Multiple sequence alignment analysis of seven *ladderlectin* genes from *S. schlegelii* was performed using the MEGA 7.0 program and visualized using GeneDoc. Simple Modular Architecture Research Tool (SMART) (http://smart.embl.de/) was used to analyze SscLLs structures and signal peptides[55]. The molecular weight (MW) and isoelectric point (pI) of protein were predicted on the EXPASY server (https://www.expasy.org/)[56]. The three-dimensional (3D) structures of SscLLs were constructed using AlphaFold3 (https://alphafold.com/) and visualized using Phyre2 (http://ww.sbg.bio.ic.ac.uk/phyre2)[57,58]. In addition, VISTA tools (https://genome.lbl.gov/vista/index.shtml) was used to compare the upstream regulatory region sequences of *ladderlectin* in different species[59].

Based on the *S. schlegelii ladderlectin* sequences, the open reading frame (ORF) of *SscLL3604* and *SscLL3605* were amplified using the specific primers (listed in Supplementary Table S4) designed by the IDT website (https://sg.idtdna.com/pages). Then, the PCR amplification products were purified using a Gel Extraction kit (CW2302M, CWBIO, Jiangsu), and ligated to pMD-19T Vector (6013, Takara, Japan) for Sanger sequencing.

Subcellular localization of SscLLs

Xho I and *Sac* II restriction sites were added to the specific primers of sSscLL-Fw and -Rv (listed in Supplementary Table S4) to facilitate the amplification of *SscLL*s, and the resulting amplicons were subsequently double-digested with *Xho* I and *Sac* II to generate sticky ends. Similarly, the pEGFP-N1 plasmid (VT1110, YouBio, Changsha) and the pDsRed2-N1 plasmid (VT1098, YouBio, Changsha) were linearized using the same restriction enzymes. The *SscLL*s fragments were then ligated into the linearized pEGFP-N1 vector and pDsRed2-N1 vector employing T4 ligase (AG11810, Accurate Biology, Changsha) individually, constructing the eukaryotic expression vectors (pEGFP-N1-SscLL3604 and pDsRed2-N1-SscLL3605), which were then transformed into the Trans5α Chemically Competent Cell (CD201-01, TransGen Biotech, Beijing). The recombinant plasmids were extracted by EndoFree Mini Plasmid Kit II (DP118, TIANGEN, Beijing). HEK293T cells were inoculated into a 24-well cell culture plate (N803024, CELLPRO, Suzhou) and cultured until the cell density was close to 80–90%. Then, recombinant pEGFP-N1-SscLL3604 and recombinant pDsRed2-N1-SscLL3605 were transfected into HEK293T cells with lipofectamine 3000 Reagent (L3000001, Thermo Fisher, USA), respectively. 24 h post-transfection, all cells were fixed in 4% PFA for 30 min, followed by a 20-min DAPI staining. The resulting fluorescence was captured using a fluorescence microscope (Leica, Germany) across various channels.

In situ hybridization (ISH), Immunohistochemistry (IHC) and Immunofluorescence (IF)

ISH was carried out after embedding the testis at different developmental stages including the regressed stage, regenerating stage, and spermatogenesis stage in paraffin, and the experiments were performed as previously described[60]. The RNA probes of *SscLL*s were amplified from testicular cDNA using specific primers listed in Supplementary Table S4, and the probes were synthesized using the DIG RNA Labeling Kit (11585614910, Roche, Switzerland). Finally, the results were observed by AZ100 (Nikon, Tokyo, Japan).

IHC was performed to detect the location of SscLLs at the protein level. The testis tissue sections underwent deparaffinization and rehydration, followed by incubation in 3% (v/v) hydrogen peroxide solution in methanol to block the endogenous peroxidase activity, antigen retrieval was performed using sodium citrate solution (C1032, Solarbio, Beijing). The sections were blocked with normal goat serum (SL038, Solarbio, Beijing) for 1.5 h at room temperature. Anti-rSscLL mouse polyclonal antibody (1:200), diluted in normal goat serum, was then applied and incubated overnight at 4 °C. After three washes with PBST, sections were treated with HRP-conjugated goat anti-mouse IgG (1:500, CW0102S, CWBIO, Jiangsu) for 1 h at room temperature. The staining process was completed using the Ultrasensitive horseradish the catalase DAB color kit (C510023, Sangon Biotech, Shanghai) in the dark for 3 min, followed by termination of the reaction with PBST. Finally, the tissues were counterstained with hematoxylin (G1080, Solarbio, Beijing), dehydrated through a gradient of ethanol, mounted with neutral balsam (G8590, Solarbio, Beijing), and observed microscopically with photographic documentation.

The protocols for IF and IHC were identical, with the exception that after incubation with the anti-rSscLL mouse polyclonal antibody (1:200, diluted in normal goat serum), the samples were incubated with Goat Anti-Mouse IgG/FITC secondary antibody (SF131, Solarbio, Beijing) for 1 h at room temperature in the absence of light. Subsequently, the samples were treated with Antifade Mounting Medium with DAPI (P0131, Beyotime, Shanghai), and the results were then photographed using a fluorescence microscope (Leica, Germany). Additionally, a polyclonal antibody against fish Vasa (GTX128306, GeneTex, USA), a YF® 594 Goat Anti-Mouse IgG (H&L) (Y6106L, UElandy, Suzhou) and a YF® 488 Goat Anti-Rabbit IgG (H&L) (Y6105L, UElandy, Suzhou) were purchased for detecting the binding of rSscLLs to ovarian cells.

Testis tissue block culture and *SscLL*s knockdown of *S. schlegelii*

According to the sequence characteristics of *SscLL3604* and *SscLL3605*, specific siRNAs targeting their coding sequences (CDS) were designed and synthesized by Sangon Biotech, with the detailed sequences provided in Supplementary Table S4.

For the culture of testis tissue blocks, a 1.5% agarose solution was prepared and sterilized via autoclaving at 121 °C. The agarose was shaped into small round pieces with a diameter of approximately 1 cm and placed in a 12-well cell culture plate. Concurrently, cellulose acetate membranes were cut to fit over the agarose, immersed in Penicillin-Streptomycin Solution (c3420-0100, VivaCell, Shanghai) overnight, and then placed on the agarose. Testis from *S. schlegelii* was dissected and washed six times in PBS to eliminate blood clots and adjacent membrane tissue. Subsequently, the testis was cut into approximately 3 mm^3 pieces and placed on the cellulose acetate membrane. Meanwhile, L-15 medium was substituted with a complete medium (containing 10% FBS, 1% Penicillin-Streptomycin Solution, 1% nonessential amino acids, 1% sodium pyruvate, 1% Glutamine, and 1% bFGF), followed by siRNA transfection after 12 h of stabilization in a 24 °C incubator.

For siRNA transfection, three groups were set up, the negative control group (NC), the *SscLL3604* knockdown group, and the *SscLL3605* knockdown group. The detailed method was based on previous descriptions[19,61–65]. Briefly, the transfection complex was prepared first, mixture 1 consisted of 50 μL L-15 medium and 2 μL lipofectamine 3000 Reagent, while mixture 2 included 50 μL L-15 medium and 2 μg siRNA (NC-siRNA for NC group, 3604-siRNA for *SscLL3604* knockdown group, and 3605-siRNA for *SscLL3605* knockdown group). After a 5-min incubation at room temperature, mixture 2 was combined with mixture 1 and gently mixed for 20 min to form the transfection complex. This complex was then slowly introduced into the tissue block culture system, and fresh L-15 complete medium was added after 6 h. Finally, tissue blocks were randomly selected for freezing at −80 °C with liquid nitrogen for RNA extraction and cDNA synthesis at the time point of 48 h post-transfection. The remaining tissue blocks were fixed in 4% PFA for H&E staining.

RNA extraction, cDNA synthesis, and quantitative real-time PCR (qRT-PCR)

Total RNA from testis tissues of both the NC group and the *SscLLs* knockdown group were extracted by SparkZol Reagent Kit (AC0101-A, SparkJade, Jinan) according to the standard protocol, the RNA quality was detected by agarose gel electrophoresis, and the RNA concentration was detected by NanoPhotometer Pearl (IMPLEN). A 5× All-in-one RT MasterMix (G592, Abm, Canada) was used for reverse transcription to synthesize complementary DNA (cDNA). The qRT-PCR experiments were performed on a Light-Cycler Roche 96 instrument (Roche Applied Science, Mannheim, Germany), with the housekeeping gene *ribosomal protein L17* (*rpl17*) as the internal control to detect the efficiency of knockdown, and the primers used for qRT-PCR are listed in Supplementary Table S4. The relative expression of each gene was calculated using the comparative $2^{-\Delta\Delta Ct}$ method[66].

Preparation of recombinant SscLLs protein (rSscLLs)

*Eco*R I and *Hin*d III restriction sites were added to the specific primers of rSscLL-Fw and -Rv (listed in Supplementary Table S4) to facilitate the amplification of *SscLLs*, and the resulting amplicons were subsequently double-digested with *Eco*R I and *Hin*d III to generate sticky ends. Similarly, the pMAL-c5x plasmid (VT2063, YouBio, Changsha) was linearized using the same restriction enzymes. The *SscLLs* fragments were then ligated into the linearized pMAL-c5x vector employing T4 ligase, yielding the recombinant pMAL-c5x-SscLL3604 and pMAL-c5x-SscLL3605.

These recombinant plasmids were transformed into *E.coli* BL21 (DE3) (CD601-02, TransGen Biotech, Beijing) for protein expression, with the empty pMAL-c5x plasmid serving as a negative control. Expression of recombinant protein (rSscLL_3604 and rSscLL_3605) was induced with 0.5 mM IPTG (I8070, Solarbio, Beijing) at 28 °C for 12 h. Purification of the resultant rSscLLs was performed utilizing Dextrin Beads 6FF (SA026005, Smart-Lifesciences, Changzhou), followed by desalination through dialysis. The purified proteins were analyzed via 12.5% SDS polyacrylamide gel electrophoresis (SDS-PAGE) and visualized using Coomassie blue fast staining solution (P0017, Beyotime, Shanghai). Recombinant protein concentration was measured using the Bradford Protein Assay Kit (EC0002, SparkJade, Jinan). Subsequently, the recombinant proteins were injected subcutaneously into five mice several times. Serum samples were collected post-injection for western blot analysis, and injection continued until the target band was detected, all serum was collected and purified to get an anti-rSscLL mouse polyclonal antibody.

Carbohydrates binding assays

The direct binding affinity of rSscLL to carbohydrates was assessed using ELISA as previously described[67]. Briefly, a selection of monosaccharides and disaccharides, namely D-mannose (D813082, Macklin, Shanghai), D-galactose (D810318, Macklin, Shanghai), D-glucose (G8150, Solarbio, Beijing), D-fructose (F8100, Solarbio, Beijing), D-(+)-Trehalose dehydrate (G8570. Solarbio, Beijing), α-lactose (L8911, Solarbio, Beijing) and Sucrose (S8271, Solarbio, Beijing), were diluted to 40 μg/mL in TBS and subsequently coated onto a 96-well cell culture plate (50 μL/well) at 25 °C. The next day, the plate was blocked with BSA (10 mg/mL diluted in TBS, A8010, Solarbio, Beijing) and washed with TBST (TBS containing 0.05% Tween-20). Recombinant proteins were then diluted with 1 mg/mL BSA (in a concentration gradient from 25 to 0 μg /mL), and incubated at room temperature for 3 h. Subsequently, anti-rSscLL mouse polyclonal antibody (1:5000, in 1 mg/mL BSA) and HRP-conjugated goat-anti-mouse IgG (1:8000, in 1 mg/mL BSA, CW0102S, CWBIO, Jiangsu) were added and incubated for 1 h respectively. Following these incubations, 100 μL of TMB single-component substrate solution (PR1200, Solarbio, Beijing) was added to each well and allowed to react for 5 min at room temperature, after which 100 μL of 1 M H_2SO4 was added to stop the reaction. The OD450 was measured using a microplate reader and recorded. Carbohydrate binding curves were generated based on the varying OD450 according to different protein concentrations. BSA and pMAL-c5x protein served as negative controls.

Sperm collection, isolation of ovarian cells, and incubation of rSscLL with ovarian cells

For sperm collection, male fish (body length: 24.8 ± 1.5 cm, body weight: 369.9 ± 43.1 g) were anesthetized using MS-222, and the testis were subsequently dissected. The vas deferens at the anterior end of the testis contain a substantial volume of mature semen. Gently squeeze the vas deferens and store the collected semen at 4 °C until incubation assays.

Ovarian cells of *S. schlegelii* were isolated via trypsin digestion. The female fish (body length: 26.5 ± 1.1 cm, body weight: 536.2 ± 81.2 g) was dissected under sterile conditions to obtain the ovary, which was immediately placed into PBS containing 1% Penicillin-Streptomycin Solution, undergoing at least six washes to eliminate blood and impurities on the ovary surface. The ovary was then cut into pieces with a volume of no more than 1 mm^3 and transferred to L-15 medium (C3070-0500, VivaCell, Shanghai) containing 0.25% trypsin (15090046, Gibco, USA), followed by shaking at room temperature to obtain a single-cell suspension. To inhibit the digestion process, 1 mL of Certified Fetal Bovine Serum (FBS, c04001-50, VivaCell, Shanghai) was added to the medium. Undigested tissue mass was filtered out using a 100 μm cell strainer (BS-100-XBS, Biosharp, Hefei), and the ovarian cells were pelleted by centrifugation at 100 g for 10 min and then resuspended in L-15 medium.

The ovarian cells were incubated with rSscLL protein at a concentration of 20 μg/mL in a 600 μL incubation system at 13 °C for 12 h, with pMAL-c5x protein serving as the negative control. Following incubation, the supernatant containing unbound proteins was discarded by centrifugation at 3000 rpm. The ovarian cells were then washed twice with PBS before subsequent treatment according to different experimental requirements.

To further elucidate the role of SscLLs in sperm binding to ovarian cells, a total of 10^7 sperm were incubated with anti-rSscLL mouse polyclonal antibody (40 μg/mL), D-fructose (80 μg/mL), D-galactose (80 μg/mL), and D-mannose (80 μg/mL) at 13 °C for 12 h. Unbound antibody and carbohydrates were removed by centrifugation, and the sperm were washed twice with PBS. Subsequently, the sperm mitochondria were labeled with Rhodamine 123 (C2007, Beyotime, Shanghai) to enable fluorescence microscopy[68]. The treated sperm were then co-incubated with ovarian cells at 24 °C for 48 h. After incubation, the L-15 culture medium was removed, and the cells were washed with PBS. Fluorescence was observed under a microscope to assess sperm binding to ovarian cells. Quantitative detection of sperm bound to ovarian cells was performed using WB analysis with anti-SPAM1 antibody.

Western blot (WB)

For WB, the procedures were conducted as previously described[19]. Briefly, proteins were extracted from tissues using RIPA buffer (R0010, Solarbio, Beijing), and the protein concentration was quantified with the Bradford Protein Assay Kit (EC0002, SparkJade, Jinan). The proteins were

subsequently detected using 12.5% SDS-PAGE and visualized with Coomassie blue fast staining solution (P0017, Beyotime, Shanghai). Following electrophoresis, the proteins were transferred to a PVDF membrane (IPFL00010, Millipore, USA), blocked with 5% non-fat powdered milk (D8340, Solarbio, Beijing) diluted in TBST, and incubated overnight at 4 °C with anti-rSscLL mouse polyclonal antibody (1:1000 dilution in TBST with 5% non-fat powdered milk). The membrane was then washed six times with TBST and incubated at room temperature for 1 h with HRP-conjugated goat-anti-mouse IgG (1:4000, dilution in 5% non-fat powdered milk, CW0102S, CWBIO, Jiangsu). Finally, the membrane was treated with ECL super chemiluminescence solution (ED0015, SparkJade, Jinan), and the results were analyzed using a luminescence imaging analyzer. Additionally, an anti-β-actin monoclonal antibody (CW0264M, CWBIO, Jiangsu) and an anti-MBP antibody (ab119994, Abcam, England) were purchased for detecting the sperm protein and the rSscLLs protein.

Statistics and reproducibility

All experiments reported in this study were replicated at least three times. Statistical analyses were performed using GraphPad Prism 8 (GraphPad Software, San Diego, CA, USA), employing a two-tailed Welch's *t* test to assess differences between groups, with $P < 0.05$ indicating statistical significance. Sample sizes were determined based on conventional research experience and ensured statistical significance. For the qRT-PCR, the relative expressions of *SscLL*s, *comt*, *cystatin*, and *insl3* post-knockdown were normalized to *rpl17*[69]. For the in vivo experiment, at least 1000 embryos were examined for each female, and the results are presented as mean ± SD. All data collected during the study were included in the analyses. Data were reviewed for completeness and accuracy, and no exclusions were made based on predefined criteria for data quality or validity. Therefore, the dataset used for analysis is identical to the dataset collected.

Reporting summary

Further information on research design is available in the Nature Portfolio Reporting Summary linked to this article.

Data availability

All relevant data are available with this publication and its supplementary files, with uncropped gel and western blot images in Supplementary Figs. 7 and 8. The source data underlying the graphs presented in this paper are available in Supplementary Data. The plasmids generated here are available from Addgene: pEGFP-N1-SscLL3604 238059, pDsRed2-N1-SscLL3605 238060, pMAL-c5x-SscLL3604 238057, pMAL-c5x-SscLL3605 238058. All other data are available from the corresponding authors on reasonable request.

Received: 19 September 2024; Accepted: 8 April 2025;
Published online: 17 April 2025

References

1. Brown, G. D., Willment, J. A. & Whitehead, L. C-type lectins in immunity and homeostasis. *Nat. Rev. Immunol.* **18**, 374–389 (2018).
2. Dambuza, I. M. & Brown, G. D. C-type lectins in immunity: recent developments. *Curr. Opin. Immunol.* **32**, 21–27 (2015).
3. Lindenwald, D. L. & Lepenies, B. C-Type lectins in veterinary species: recent advancements and applications. *Int. J. Mol. Sci.* **21**, 5122 (2020).
4. Goluboff, E. T., Mertz, J. R., Tres, L. L. & Kierszenbaum, A. L. Galactosyl receptor in human testis and sperm is antigenically related to the minor C-type (Ca^{2+}-dependent) lectin variant of human and rat liver. *Mol. Reprod. Dev.* **40**, 460–466 (1995).
5. Dong, C.-H., Yang, S.-T., Yang, Z.-A., Zhang, L. & Gui, J.-F. A C-type lectin associated and translocated with cortical granules during oocyte maturation and egg fertilization in fish. *Dev. Biol.* **265**, 341–354 (2004).
6. Moy, G., Springer, S., Adams, S., Swanson, W. & Vacquier, V. Extraordinary intraspecific diversity in oyster sperm bindin. *Proc. Natl. Acad. Sci. USA* **105**, 1993–1998 (2008).
7. Kim, H. et al. Immunohistochemical study of galectin-3 in mature and immature bull testis and epididymis. *J. Vet. Sci.* **9**, 339–344 (2009).
8. Mei, S., Chen, P., Lee, C. L., Zhao, W. & Chiu, P. C. N. The role of galectin-3 in spermatozoa-zona pellucida binding and its association with fertilization in vitro. *Mol. Hum. Reprod.* **25**, 458–470 (2019).
9. Block, A. S., Saraswati, S., Lichti, C. F., Mahadevan, M. & Diekman, A. B. Co-purification of Mac-2 binding protein with galectin-3 and association with prostasomes in human semen. *Prostate* **71**, 711–721 (2011).
10. Jensen, L. E., Thiel, S., Petersen, T. E. & Jensenius, J. C. A Rainbow Trout Lectin with Multimeric Structure. *Comp. Biochem. Physiol. Part B Biochem. Mol. Biol.* **116**, 385–390 (1997).
11. Young, K. M. et al. Bacterial-binding activity and plasma concentration of ladderlectin in rainbow trout (*Oncorhynchus mykiss*). *Fish. Shellfish Immunol.* **23**, 305–315 (2007).
12. Wang, W., Liu, M., Fei, C., Li, C. & Chen, J. Molecular and functional characterization of a ladderlectin-like molecule from ayu (*Plecoglossus altivelis*). *Fish. Shellfish Immunol.* **131**, 419–430 (2022).
13. Feng, C. et al. A novel ladderlectin from hybrid crucian carp possesses antimicrobial activity and protects intestinal mucosal barrier against *Aeromonas hydrophila* infection. *Fish. Shellfish Immunol.* **124**, 1–11 (2022).
14. Tang, X., Zhu, X., Liu, X., Wang, Z. & Zhang, D. A unique C-type lectin, Ladderlectin, from large yellow croaker (*Larimichthys crocea*) is involved in bacterial cell membrane damage. *Fish. Shellfish Immunol.* **136**, 108744 (2023).
15. Hoover, G. J., El-Mowafi, A., Simko, E., Kocal, T. E. & Hayes, M. A. Plasma proteins of rainbow trout (*Oncorhynchus mykiss*) isolated by binding to lipopolysaccharide from *Aeromonas salmonicida*. *Comp. Biochem. Physiol. B Biochem. Mol. Biol.* **120**, 559–569 (1998).
16. Reid, A., Young, K. M. & Lumsden, J. S. Rainbow trout *Oncorhynchus mykiss* ladderlectin, but not intelectin, binds viral hemorrhagic septicemia virus IVb. *Dis. Aquat. Org.* **95**, 137 (2011).
17. He, Y., Chang, Y., Bao, L., Yu, M. & Qi, J. A chromosome-level genome of black rockfish, *Sebastes schlegelii*, provides insights into the evolution of live birth. *Mol. Ecol. Resour.* **19**, 1309–1321 (2019).
18. Li, R. et al. Transcriptome sequencing reveals ovarian immune response and development during female sperm storage in viviparous black rockfish (*Sebastes schlegelii*). *Comparative biochemistry and physiology. Part D., Genomics Proteom.* **45**, 101050 (2022).
19. Li, R. et al. Expression analysis of ZPB2a and its regulatory role in sperm-binding in viviparous teleost black rockfish. *Int. J. Mol. Sci.* **23**, 9498 (2022).
20. Clark, G. F. The role of carbohydrate recognition during human sperm-egg binding. *Hum. Reprod.* **28**, 566–577 (2013).
21. Holmskov, U., Malhotra, R., Sim, R. B. & Jensenius, J. C. Collectins: collagenous C-type lectins of the innate immune defense system. *Immunol. Today* **15**, 67–74 (1994).
22. Chaofan, J. et al. Dissecting the dynamic cellular transcriptional atlas of adult teleost testis development throughout the annual reproductive cycle. *Development* **151**, dev202296 (2024).
23. Petit, F., Serres, C., Bourgeon, F., Pineau, C. & Auer, J. Identification of sperm head proteins involved in zona pellucida binding. *Hum. Reprod.* **28**, 852–865 (2013).
24. Amores, A., Catchen, J., Ferrara, A., Fontenot, Q. & Postlethwait, J. H. Genome evolution and meiotic maps by massively parallel DNA sequencing: spotted gar, an outgroup for the teleost genome duplication. *Genetics* **188**, 799–808 (2011).
25. Russell, S., Young, K. M., Smith, M., Hayes, M. A. & Lumsden, J. S. Cloning, binding properties, and tissue localization of rainbow trout

(*Oncorhynchus mykiss*) ladderlectin. *Fish. Shellfish Immunol.* **24**, 669–683 (2008).
26. Drickamer, K. C-type lectin-like domains. *Curr. Opin. Struct. Biol.* **9**, 585–590 (1999).
27. Zelensky, A. N. & Gready, J. E. The C-type lectin-like domain superfamily. *FEBS J.* **272**, 6179–6217 (2005).
28. Stavenhagen, K. et al. N-glycosylation of mannose receptor (CD206) regulates glycan binding by C-type lectin domains. *J. Biol. Chem.* **298**, 102591 (2022).
29. Owji, H., Nezafat, N., Negahdaripour, M., Hajiebrahimi, A. & Ghasemi, Y. A comprehensive review of signal peptides: Structure, roles, and applications. *Eur. J. Cell Biol.* **97**, 422–441 (2018).
30. O'Donnell, L., Smith, L. B. & Rebourcet, D. Sertoli cells as key drivers of testis function. *Semin. Cell Dev. Biol.* **121**, 2–9 (2022).
31. Hai, Y. et al. The roles and regulation of Sertoli cells in fate determinations of spermatogonial stem cells and spermatogenesis. *Semin. Cell Dev. Biol.* **29**, 66–75 (2014).
32. Rojas, M. & Esponda, P. Plasma membrane glycoproteins during spermatogenesis and in spermatozoa of some fishes. *J. Submicroscopic Cytol. Pathol.* **33**, 133–140 (2001).
33. Inoue, N., Ikawa, M., Isotani, A. & Okabe, M. The immunoglobulin superfamily protein Izumo is required for sperm to fuse with eggs. *Nature* **434**, 234–238 (2005).
34. Lorenzetti, D. et al. A transgenic insertion on mouse chromosome 17 inactivates a novel immunoglobulin superfamily gene potentially involved in sperm–egg fusion. *Mamm. Genome* **25**, 141–148 (2014).
35. Pausch, H. et al. A nonsense mutation in *TMEM95* encoding a nondescript transmembrane protein causes idiopathic male subfertility in cattle. *PLoS Genet.* **10**, e1004044 (2014).
36. Fujihara, Y. et al. Spermatozoa lacking Fertilization Influencing Membrane Protein (FIMP) fail to fuse with oocytes in mice. *Proc. Natl. Acad. Sci.* **117**, 9393–9400 (2020).
37. Ge, R., Li, X. & Wang, Y. Leydig cell and spermatogenesis. *Adv. Exp. Med. Biol.* **1288**, 111–129 (2021).
38. Li, Y. et al. High throughput scRNA-Seq provides insights into Leydig cell senescence induced by experimental autoimmune Orchitis: a prominent role of interstitial fibrosis and complement activation. *Front. Immunol.* **12**, 771373 (2022).
39. Zhou, R. et al. The roles and mechanisms of Leydig cells and myoid cells in regulating spermatogenesis. *Cell. Mol. Life Sci.* **76**, 2681–2695 (2019).
40. Yuan, S. et al. Sperm-borne miRNAs and endo-siRNAs are important for fertilization and preimplantation embryonic development. *Development* **143**, 635–647 (2016).
41. Mukherjee, A. G. & Gopalakrishnan, A. V. Anti-sperm Antibodies as an Increasing Threat to Male Fertility: Immunological Insights, Diagnostic and Therapeutic Strategies. *Reprod. Sci.* **31**, 1–20 (2024).
42. Zhang, G. et al. HIRA and dPCIF1 coordinately establish totipotent chromatin and control orderly ZGA in Drosophila embryos. *Proc. Natl. Acad. Sci.* **121**, e2410261121 (2024).
43. Kuo, Y. W., Li, S. H., Maeda, K. I., Gadella, B. M. & Tsai, P. S. J. Roles of the reproductive tract in modifications of the sperm membrane surface. *J. Reprod. Dev.* **62**, 337–343 (2016).
44. Zhang, Y., Zhang, W., Liu, Y., Ren, B. & Guan, Y. The impact of intracytoplasmic sperm injection versus conventional in vitro fertilization on the reproductive outcomes of couples with non-male factor infertility and frozen-thawed embryo transfer cycles. *Sci. Rep.* **14**, 20433 (2024).
45. Solovieff, N., Cotsapas, C., Lee, P. H., Purcell, S. M. & Smoller, J. W. Pleiotropy in complex traits: challenges and strategies. *Nat. Rev. Genet.* **14**, 483–495 (2013).
46. Stearns, F. W. One hundred years of pleiotropy: a retrospective. *Genetics* **186**, 767–773 (2010).
47. Camaioni, A., Klinger, F. G., Campagnolo, L. & Salustri, A. The influence of pentraxin 3 on the ovarian function and its impact on fertility. *Front. Immunol.* **9**, 2808 (2018).
48. Van Mourik, M. S., Macklon, N. S. & Heijnen, C. J. Embryonic implantation: cytokines, adhesion molecules, and immune cells in establishing an implantation environment. *J. Leucoc. Biol.* **85**, 4–19 (2009).
49. Sanguansermsri, D. & Pongcharoen, S. Pregnancy immunology: decidual immune cells. *Asian Pac. J. Allergy Immunol.* **26**, 171–181 (2008).
50. Fassler, M., Li, X. & Kaether, C. Polar transmembrane-based amino acids in presenilin 1 are involved in endoplasmic reticulum localization, Pen2 protein binding, and γ-secretase complex stabilization. *J. Biol. Chem.* **286**, 38390–38396 (2011).
51. Kawasaki, T., Shimizu, Y., Mori, T., Hiramatsu, N. & Todo, T. Development of artificial insemination techniques for viviparous black rockfish (*Sebastes schlegelii*). *Aquac. Sci.* **65**, 73–82 (2017).
52. Zhang, D., Gao, F., Jakovli, I., Zou, H. & Wang, G. T. PhyloSuite: An integrated and scalable desktop platform for streamlined molecular sequence data management and evolutionary phylogenetics studies. *Mol. Ecol. Resour.* **20**, 348–355 (2020).
53. LetunicBork Interactive Tree Of Life (iTOL): an online tool for phylogenetic tree display and annotation. *Bioinformatics* **23**, 127–128 (2007).
54. Patro, R., Duggal, G., Love, M. I., Irizarry, R. A. & Kingsford, C. Salmon provides fast and bias-aware quantification of transcript expression. *Nat. Methods* **14**, 417–419 (2017).
55. Ivica, L., Supriya, K. & Peer, B. SMART: recent updates, new developments and status in 2020. *Nucleic Acids Res.* **49**, D458–D460 (2020).
56. Duvaud, S., Gabella, C., Lisacek, F., Stockinger, H. & Durinx, C. Expasy, the Swiss Bioinformatics Resource Portal, as designed by its users. *Nucleic Acids Res.* **49**, W216–W227 (2021).
57. Abramson, J. et al. Accurate structure prediction of biomolecular interactions with AlphaFold 3. *Nature* **630**, 493–500 (2024).
58. Kelley, L. A., Mezulis, S., Yates, C. M., Wass, M. N. & Sternberg, M. J. E. The Phyre2 web portal for protein modeling, prediction and analysis. *Nat. Protoc.* **10**, 845–858 (2015).
59. Frazer, K. A., Lior, P., Alexander, P., Rubin, E. M. & Inna, D. VISTA: computational tools for comparative genomics. *Nucleic Acids Res.* **32**, W273–W279 (2004).
60. Yano, A., Nicol, B., Guerin, A. & Guiguen, Y. The duplicated rainbow trout (*Oncorhynchus mykiss*) T-box transcription factors 1, *tbx1a* and *tbx1b*, are up-regulated during testicular development. *Mol. Reprod. Dev.* **78**, 172–180 (2011).
61. Ruigrok, M. J. R., Xian, J. L., Frijlink, H. W., Melgert, B. N. & Olinga, P. siRNA-mediated protein knockdown in precision-cut lung slices. *Eur. J. Pharmaceutics Biopharmaceutics* **133**, 339–348 (2018).
62. Ewe, A. et al. Optimized polyethylenimine (PEI)-based nanoparticles for siRNA delivery, analyzed in vitro and in an ex vivo tumor tissue slice culture model. *Drug Deliv. Transl. Res.* **7**, 206–216 (2017).
63. Arany, S. et al. Pro-apoptotic gene knockdown mediated by nanocomplexed siRNA reduces radiation damage in primary salivary gland cultures. *J. Cell. Biochem.* **113**, 1955–1965 (2012).
64. Cardoso, A. L. et al. Tf-lipoplexes for neuronal siRNA delivery: A promising system to mediate gene silencing in the CNS. *J. Controlled Rel.* **132**, 113–123 (2008).
65. Taheri, N., Choi, E. L., Zhang, Y. & Hayashi, Y. Protocol for gene knockdown using siRNA in organotypic cultures of murine gastric muscle. *J. Smooth Muscle Res.* **60**, 64–71 (2024).
66. Livak, K. J. & Schmittgen, T. D. Analysis of relative gene expression data using real-time quantitative PCR and the $2^{-\Delta\Delta CT}$ method. *Methods* **25**, 402–408 (2001).
67. Huang, Y., Shi, Y., Hu, S., Wu, T. & Zhao, Z. Characterization and Functional Analysis of Two Transmembrane C-Type Lectins in Obscure Puffer (*Takifugu obscurus*). *Front. Immunol.* **11**, 436 (2020).
68. Niu, J. et al. Effects of cryopreservation on sperm with cryodiluent in viviparous black rockfish (*Sebastes schlegelii*). *Int. J. Mol. Sci.* **23**, 3392 (2022).

69. Chaofan, J. et al. Transcriptome-Wide Identification and Validation of Reference Genes in Black Rockfish (*Sebastes schlegelii*). *J. Ocean Univ. China* **20**, 654–660 (2021).

Acknowledgements

This study was financially supported by the National Natural Science Foundation of China (32370564, 32070515), the Key Research and Development Project of Shandong Province (2022ZLGX01). The funders were not involved in the design of the study and collection, analysis, and interpretation of data and in writing the manuscript.

Author contributions

Conceptualisation: Yan He, Jie Qi and Weihao Song. Investigation: Ruiyan Yang, Weihao Song, Mengda Du, Fengyan Zhang and Xiangyu Gao. Validation: Na Wang, Gongchen Liu, Fuxiang Liu and Hang Zhang. Formal analysis and visualisation: Ruiyan Yang, Hao Sun and Tianci Nie. Writing – original draft: Ruiyan Yang. Writing – review & editing: all authors. All authors reviewed the results and approved the final version of the manuscript.

Competing interests

The authors declare no competing interests.

Additional information

Supplementary information The online version contains supplementary material available at https://doi.org/10.1038/s42003-025-08055-2.

Correspondence and requests for materials should be addressed to Weihao Song or Yan He.

Peer review information *Communications Biology* thanks the anonymous reviewers for their contribution to the peer review of this work. Primary Handling Editors: Frank Avila and Johannes Stortz. A peer review file is available.